

# Region-specific response of central microglial cells to sciatic nerve demyelination through sensory and motor pathways

Shuang Wu\*, Yuxin Su\*, Yuqing Wang, Jia Wang, Dongsheng Xu, Yihan Liu, Kunwu Yang, Junhong Gao, Jingjing Cui and Wanzhu Bai

Institute of Acupuncture and Moxibustion, China Academy of Chinese Medical Sciences, Beijing, PR China

\*The first two authors contributed equally to this work

**Summary.** Peripheral nerve injury can cause changes in microglial cells on the spinal dorsal and ventral horns. This region-specific response implies that central microglial cells could be activated through both sensory and motor pathways. In order to further determine how peripheral nerve injury activates central microglial cells through neural pathways, the sciatic nerve was selected as the target for neural tract tracing and demyelination. Firstly, we used cholera toxin subunit B (CTB) to map the central sensory and motor territories of the sciatic nerve. Secondly, we applied lysophosphatidylcholine to establish the model of sciatic nerve demyelination and examined the distribution of activated microglial cells via immunofluorescence with ionized calcium-binding adapter molecule 1. It was shown that CTB labeling included the transganglionically labeled sensory afferents and retrogradely labeled somata of motor neurons along the sensory and motor pathways of the sciatic nerve ipsilateral to the injection, in which sensory afferents terminated on the gracile nucleus, Clarke's nucleus, and spinal dorsal horn, while motor neurons located on the spinal ventral horn. Consistently, after sciatic nerve demyelination, the activated microglial cells were observed in the same territories as CTB-labeling, showing shortened processes and enlarged cell bodies. These results support the idea that central microglia might be activated by signals from the demyelinated sciatic nerve through both sensory and motor pathways.

**Key words:** Peripheral nerve injury, Demyelination, Microglial cells, Sciatic nerve, Lysophosphatidylcholine, Cholera toxin subunit B

*Corresponding Author:* Jingjing Cui and Wanzhu Bai, Institute of Acupuncture and Moxibustion, China Academy of Chinese Medical Sciences, 16 Nanxiaojie of Dongzhimennei, Beijing, 100700, PR China. e-mail: cuijing101@163.com and wanzhubaisy@hotmail.com www.hh.um.es. DOI: 10.14670/HH-18-681

## Introduction

Peripheral nerve injury can cause the activation of microglial cells in the central nervous system (Eriksson et al., 1993; Rotterman et al., 2019; Pottorf et al., 2022). A great number of researchers have focused their observations on the central microglial activation induced by peripheral nerve injury, which may be closely related to colony-stimulating factor 1 (CSF1) (Köbbert and Thanos, 2000; Beggs and Salter, 2007; Rotterman et al., 2019; Nishihara et al., 2020). Considering that activated microglial cells are distributed on both spinal dorsal and ventral horns in a region-specific pattern (Eriksson et al., 1993; Rotterman et al., 2019; Pottorf et al., 2022), this implies that central microglial cells might be activated through both sensory and motor pathways (Köbbert and Thanos, 2000; Beggs and Salter, 2007; Nishihara et al., 2020).

To provide detailed information for determining how peripheral nerve demyelination activates microglia through sensory or motor pathways, the rat sciatic nerve was selected for neural tract tracing and demyelination. On the one hand, cholera toxin subunit B (CTB) was used to map the central sensory and motor territories of the sciatic nerve. After peripheral application, CTB can transganglionically label the central sensory terminals and retrogradely label the motor neurons in the central nervous system (Rivero-Melián et al., 1992; Beggs and Salter, 2007; Xu et al., 2021). On the other hand, lysophosphatidylcholine (LPC) was applied to establish the experimental model of sciatic nerve demyelination (Inoue et al., 2008; Nishimoto et al., 2015; Matsuoka et al., 2018). Using this model, we aimed to figure out the distribution of activated microglial cells after modeling

**Abbreviations.** CTB, cholera toxin subunit B; Iba1, ionized calcium-binding adapter molecule 1; LPC, lysophosphatidylcholine; PB, phosphate buffer.



by using immunofluorescence with ionized calcium-binding adapter molecule 1 (Iba1) and CSF1 (Köbber and Thanos, 2000; Beggs and Salter, 2007; Rotterman et al., 2019; Nishihara et al., 2020), further demonstrating the spatial correlation of activated microglial cells and neurons in detail.

By comparing the central sensory and motor territories of the sciatic nerve mapped with CTB, we determined whether central microglial cells were activated by sciatic nerve demyelination through both sensory and motor pathways. This study gives further insight into the central mechanisms of peripheral nerve demyelination and the possible neural elements involved in activating microglia.

## Materials and methods

### Animals

Fifteen young adult male Sprague Dawley rats (8-10 weeks, weight 220±30 g) were used in this study. Animals (license No. SCXK (JING) 2019-0010) were provided by the National Institutes for Food and Drug Control. All animals were allowed free access to food and water and housed in a 12h light/dark cycle with controlled temperature and humidity. This study was approved by the ethics committee of the Institute of Acupuncture and Moxibustion, China Academy of Chinese Medical Sciences, and carried out in accordance with the National Institutes of Health Guide for the Care and Use of Laboratory Animals (National Academy Press, Washington DC, USA).

### Microinjection, transection or crush injury of the sciatic nerve

The neural tracer CTB was used in this study to map the distribution of sciatic sensory afferents and motor neurons (n=3) (Wu et al., 2021). In surgical approaches, anesthesia was induced using isoflurane. The surgical site was sterilized and opened, and the sciatic nerve on the left side was exposed between the gluteus superficialis and the biceps femoris muscles through blunt dissection of the connective tissue. Then, a total of 0.5 µl of 1% CTB (#104, List Biological Labs, Campbell, CA, USA, dissolved with sterile double distilled water) solution was slowly injected under the epineurium of the sciatic nerve with a 30-gauge Hamilton syringe into the proximal part of the sciatic nerve. The incision was closed by suture.

Similar to the CTB injection procedure, the model of chemical demyelination was established following injection of LPC into the rat sciatic nerve (n=6). The difference was that a total of 5 µl of 2% LPC (L4128, Sigma, USA, dissolved with sterile saline) was injected. Besides, for the model of mechanical damage was established with either transecting the sciatic nerve or manually clamping it between the smooth-surfaced tips of forceps (F31023-12, RWD, China) for 30 seconds

twice (n=3). Here, all efforts were made to minimize the number of animals used in this study.

### Perfusions

The rats with CTB injection were sacrificed after a survival period of three days, while those with LPC injection, transection and crush injury were allowed to survive for seven days. Following deep anesthesia with an overdose of tribromoethanol solution (250 mg/kg) via intraperitoneal injection, the rats were transcardially perfused with 0.9% sodium chloride solution (100 mL) followed by 4% paraformaldehyde in 0.1 mol/L (M) phosphate buffer (PB, pH 7.4, 300 mL). After perfusion, the brain, spinal cord and sciatic nerve were carefully dissected out and post-fixed for 2h, then cryopreserved in 0.1 M PB containing 25% sucrose at 4°C overnight.

### Sectioned tissue preparations

Serial coronal sections of the brain and transverse sections of the spinal cord were cut at a thickness of 40 µm on a sliding microtome system (Yamato, REM-710, Japan) and collected in order in a six-hole Petri dish with 0.1 M PB (pH 7.4). Meanwhile, serial horizontal sections of the sciatic nerve were cut at a thickness of 60 µm. The sites of neural labeling and glial labeling in the brain and spinal cord were judged according to *The rat brain in stereotaxic coordinates* (Paxinos and Watson, 2007).

### Immunohistofluorescence staining

Immunohistofluorescence staining was carried out to demonstrate the CTB labeling. The sections were incubated in blocking solution (3% normal donkey serum and 0.5% Triton X-100 in 0.1 M PB) for 1 hour at room temperature and then changed into the solution containing primary antibody of goat anti-CTB (1:1000, #703, List Biological Labs, Campbell, USA) with 1% normal donkey serum and 0.5% Triton X-100 in 0.1 M PB for overnight at 4°C. After washing three times (5 min each) with 0.1 M PB (pH 7.4), the sections were incubated with the solution containing the second antibody of Alexa Fluor (AF) 594 donkey anti-goat IgG (1:500, A11058, Thermo Fisher, Waltham, USA) and NeuroTrace 500/525 Green Fluorescent Nissl Stain (1:1000, N21480, Thermo Fisher, Waltham, USA) with 1% normal donkey serum and 0.5% Triton X-100 in 0.1 M PB for 2 hours at room temperature. Finally, the sections were rinsed with 0.1 M PB, mounted onto slides (Superfrost), air-dried, and cover slipped with 50% glycerin.

A similar staining process was performed on the experimental models to certify the sciatic nerve demyelination and to label microglia activation. The difference being that the primary antibodies of mouse anti-myelin basic protein (MBP, 1:500, 83683S, Cell Signaling Technology, MA, USA), rabbit anti-

neurofilament 200 (NF200, 1:5000, N4142, Sigma, USA), mouse anti-Iba1 (1:1000, ab283319, Abcam, Hong Kong Administrative Region, China), and rabbit anti-CSF1 (1:100, ab233387, Abcam, Hong Kong

Administrative Region, China) were used and followed with the second antibody of AF594 donkey anti-mouse IgG (1:500, A21203, Thermo Fisher, Waltham, USA), AF488/594 donkey anti-rabbit IgG (1:500, A21206/

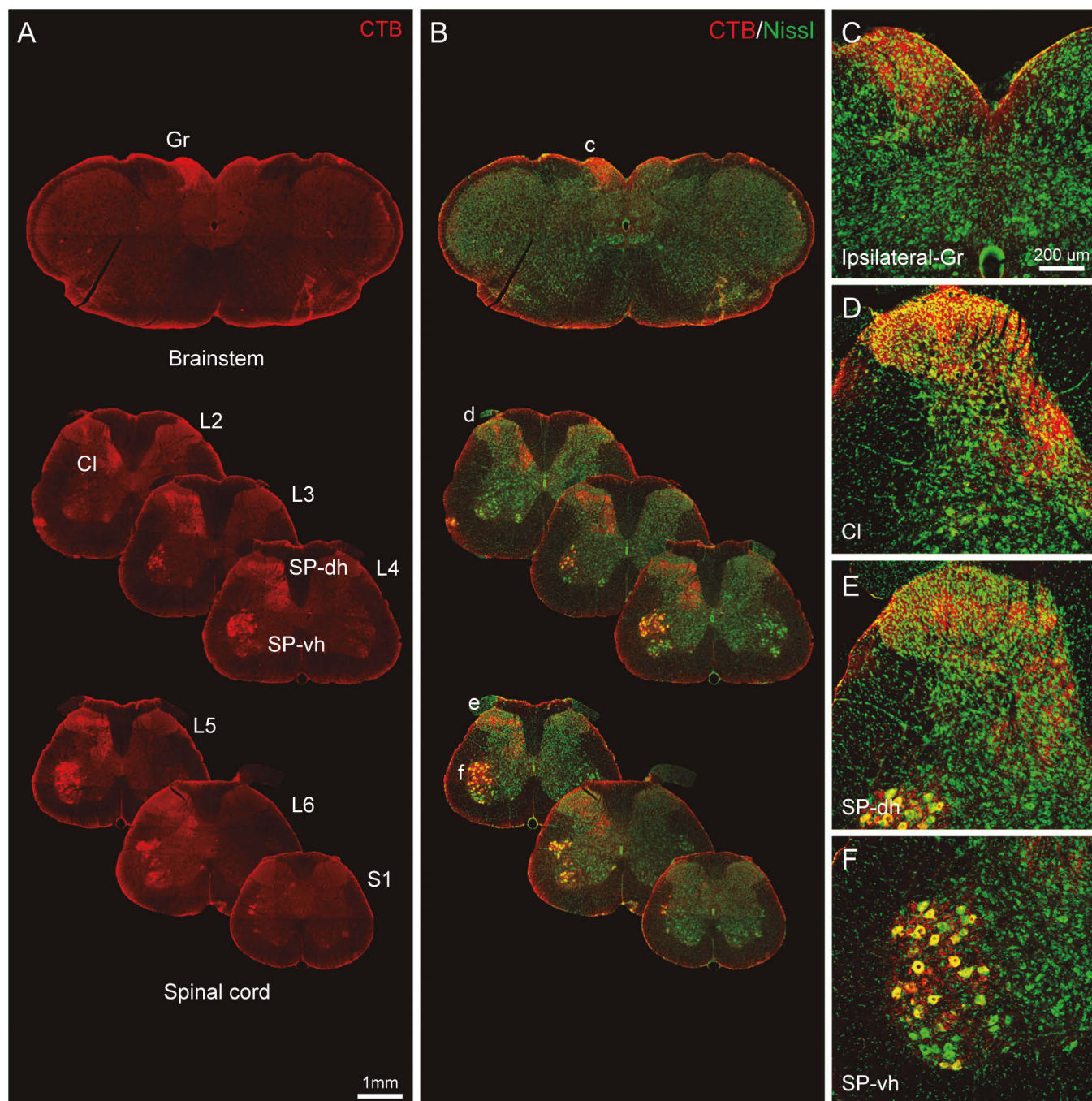


**Fig. 1.** The central sensory and motor territories of the sciatic nerve to be labeled with cholera toxin subunit B (CTB). **A.** A series of representative images through the brain stem and six levels of the spinal cord showing the distribution of transganglionically labeled axon terminals in the gracile nucleus (Gr), Clarke's nucleus (Cl), and spinal dorsal horn from lumbar (L) 2 to L6 segments, as well as retrogradely labeled motor neuronal somata in the spinal ventral horn from L3 to sacral (S) 1 segments. All CTB labeling is located on the ipsilateral side of injection. **B.** Figure A with the background of fluorescent Nissl staining. **C-F.** Magnified images from the corresponding regions of c, d, e, and f in Figure B separately showing the labeled axon terminals and neurons in detail. Same scale for A and B, for C-F.

A21207, Thermo Fisher, Waltham, USA) and NeuroTrace 500/525 Green Fluorescent Nissl Stain (1:1000, N21480, Thermo Fisher, Waltham, USA) in 1% normal donkey serum and 0.5% Triton X-100 in 0.1 M PB correspondingly.

#### Microscopy and statistical analysis

**Microscopy and images.** The samples were scanned with the VS120 Virtual Slide System (Olympus, Japan). Accordingly, the representative regions of the gracile nucleus, Clarke's nucleus, and spinal dorsal and ventral horns were selected to further view and record with a confocal imaging system (FV1200, Olympus, Japan). All images were analyzed using Olympus Image Processing Software and processed using Adobe Photoshop CS5 and Adobe Illustration CS5 (Adobe Systems, San Jose, CA, USA). Three-dimensional reconstruction of the microglia was performed using Imaris 7.7.1 software (www.bitplane.com) as previously described (Wright and Horn, 2016; Wang et al., 2020, 2022). Care was taken so as not to remove any data from the images.

**Statistical analysis.** Three low-power images of every sixth section from the brainstem (8-10 sections) and spinal cord (40-45 sections) of three rats were used to calculate the area ratio of Iba1 labeling by using Image J (National Institutes of Health developed imaging processing program, Bethesda, Maryland,

USA), respectively. All data were expressed as mean  $\pm$  standard error (SEM) and processed with GraphPad Prism version 8.2.1 (La Jolla, CA, USA). The two-tailed t-test was applied for the comparison between two groups.  $P < 0.05$  was considered statistically significant.

## Results

### Distribution of neural labeling with CTB

Following the injection of CTB into the sciatic nerve, neural labeling was observed on the brain stem and spinal cord ipsilateral to the injection side. Among this labeling, the transganglionically labeled sensory terminals distributed on the gracile nucleus, Clarke's nucleus, and spinal dorsal horn from lumbar (L) 2 to L6 segments, while the retrogradely labeled motor neuronal somata were detected in the spinal ventral horn from L3 to sacral (S) 1 segments (Fig. 1). It was clear that the distribution of central sensory terminals and motor neurons associated with the sciatic nerve was in a region-specific pattern.

### Distribution of activated microglial cells

The distribution of activated microglial cells was examined seven days after sciatic nerve demyelination (Fig. 2). Compared to normal rats, the injured rats with

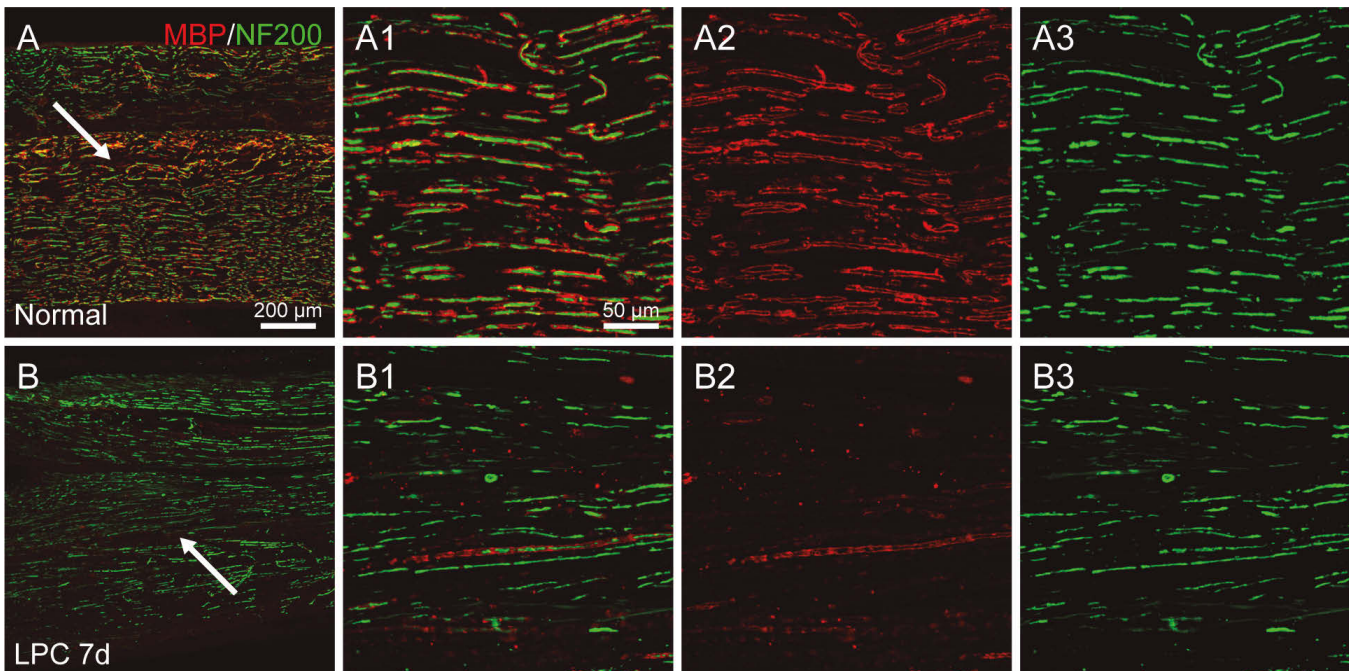


**Fig. 2.** Distribution characteristics of myelin sheath and nerve fibers in the normal and lysophosphatidylcholine injured sciatic nerve on the 7th day. **A, B.** Representative images from normal (**A**) and lysophosphatidylcholine injured (**B**) sciatic nerve of MBP+ myelin sheath and NF200+ nerve fiber on the 7th day. **A1, B1.** Magnified photographs from panels A-B (arrow-indicated regions). **A2-B2, A3-B3.** The images separated from Figures A-B show the MBP+ myelin sheath (**A2-B2**) and NF200+ nerve fiber (**A3-B3**) independently.

### Microglial activation to nerve injury

LPC had decreased MBP+ myelin sheath on the sciatic nerve (Fig. 2). All activated microglial cells were found on the ipsilateral side of the LPC injury (Fig. 3). Consistent with the topographic map of neural labeling with CTB, the activated microglial cells were also observed on the gracile nucleus, Clarke's nucleus, and spinal dorsal and ventral horns within similar regions and spinal segments but were less detected outside these regions (Fig. 3).

In addition, the morphological characteristics of activated and resident microglial cells were compared between both sides of the gracile nucleus, Clarke's nucleus, and spinal dorsal and ventral horns with images at higher magnification (Fig. 4). On the uninjured side, the

resident microglial cells were in "resting" state with small cell bodies and fine processes, which appeared to be spatially independent of neurons (Fig. 4). In contrast, on the LPC injured side, numerous activated microglial cells gathered together within injured territories and displayed shortened processes and enlarged somata (Fig. 4). Within the involved sensory regions, the activated microglial cells located close to local neurons (speculated secondary sensory neurons or local interneurons) but only attached neurons with their processes (Fig. 4). However, within the involved motor regions, the activated microglial cells intimately adhered to the injured motor neurons with faded Nissl labeling (Fig. 4).

Statistical analysis showed that the area ratio of

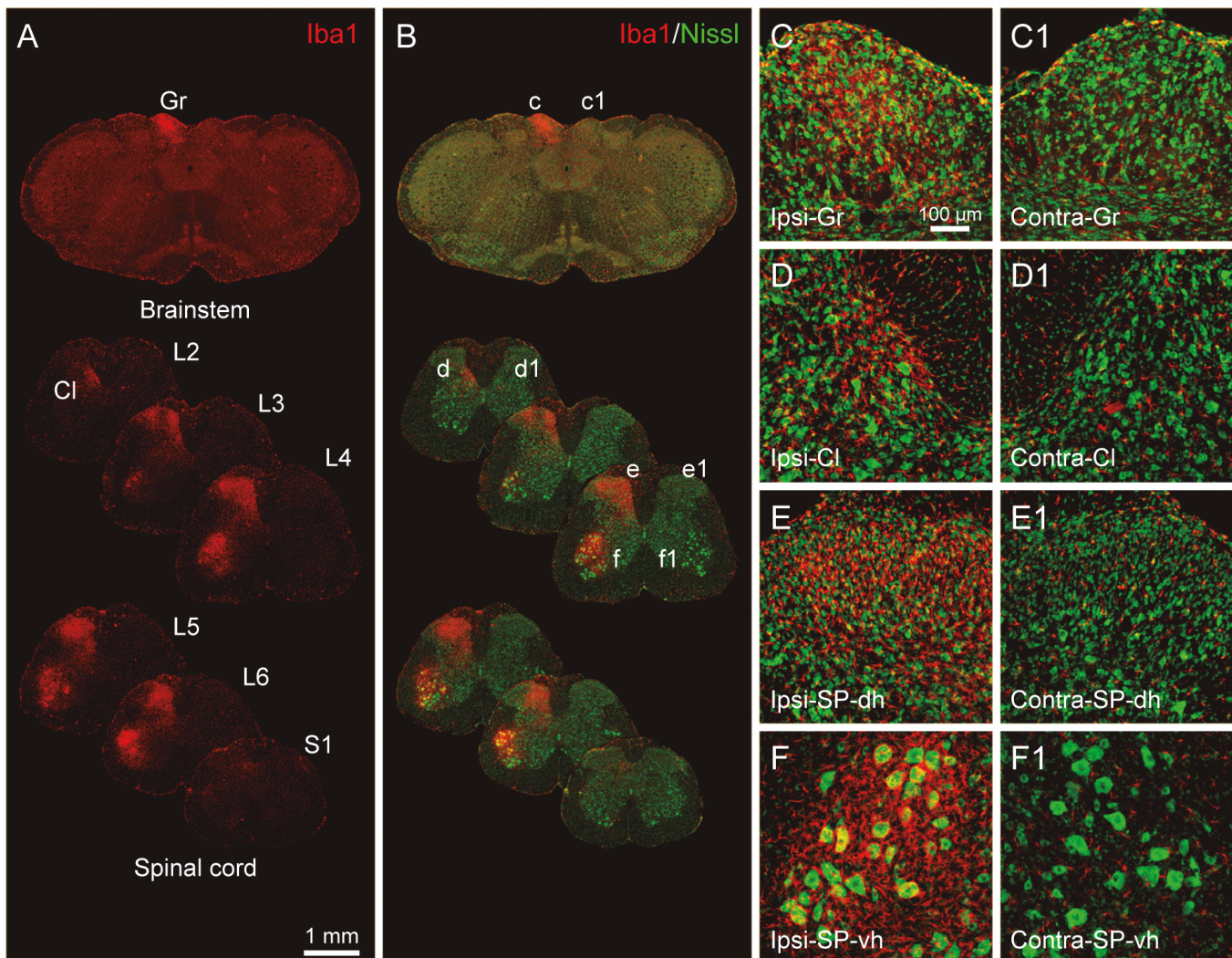


**Fig. 3.** Region-specific response of central microglial cells to sciatic nerve demyelination with lysophosphatidylcholine. **A.** A series of representative images through the brain stem and six levels of the spinal cord showing the distribution of activated and resident microglial cells on both sides of the gracile nucleus (Gr), Clarke's nucleus (Cl), and spinal dorsal horn (SP-dh) and spinal ventral horn (SP-vh), respectively. All activated microglial cells are located on the ipsilateral (ipsi) side of injection. **B.** Figure A with the background of fluorescent Nissl staining. **C-F, C1-F1.** Magnified images from the corresponding regions of c-f and c1-f1 in Figure B separately show the activated microglial cells on the ipsilateral side (**C-F**) and resident microglial cells on the contralateral side (**C1-F1**) respectively. Iba1: ionized calcium-binding adapter molecule 1. Same scale for A and B, for C-F and C1-F1.

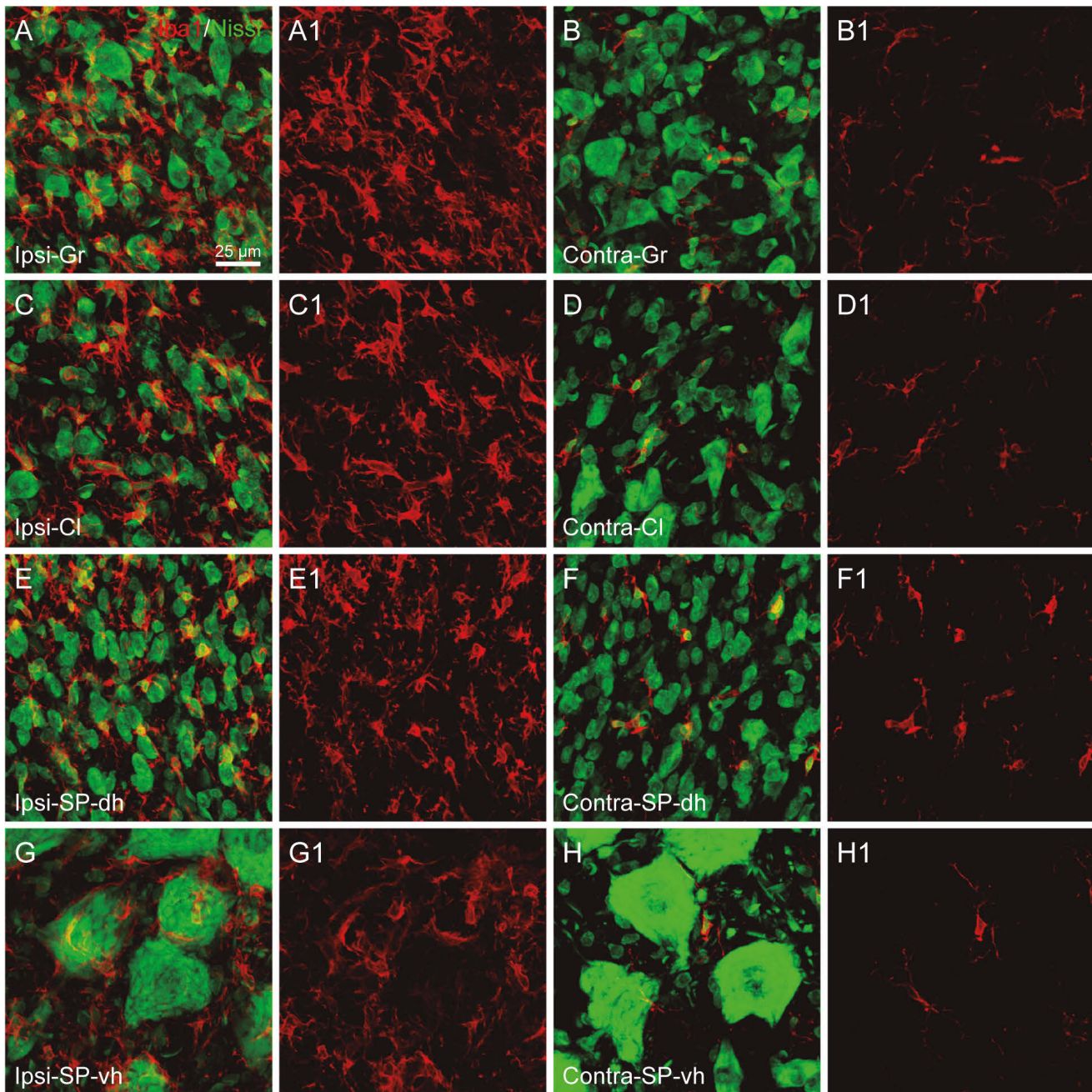


**Fig. 4.** Regional differences in microglial cells between the bilateral central sensory and motor territories of the lysophosphatidylcholine injured sciatic nerve. **A-H.** Representative images from bilateral sides of the gracile nucleus (**A, B**), Clarke's nucleus (**C, D**), spinal dorsal horn (**E, F**), and spinal ventral horn (**G, H**) showing activated microglial cells on the ipsilateral side of lysophosphatidylcholine injury (**A, C, E, G**) and resident microglial cells on the contralateral side of injury (**B, D, F, H**). **A1-H1.** Images separated from Figures A-H show the microglial cells independently. **I.** Quantitative analysis of the area ratio of Iba1+ microglial cells (n=3 rats, \*\*\*\* $P < 0.0001$ , \*\*\* $P < 0.001$ ). Iba1: ionized calcium-binding adapter molecule 1. Same scale for all images.

Iba1+ microglia cells on the LPC injured side of the gracile nucleus, Clarke's nucleus, and spinal dorsal and ventral horns was significantly higher than those of the corresponding regions on the contralateral side

( $P < 0.0001$  and  $P < 0.001$ , respectively, Fig. 4I). In parallel to the areas of microglial activation, as above mentioned, the expression of CSF1 was also simultaneously upregulated (Fig. 5).

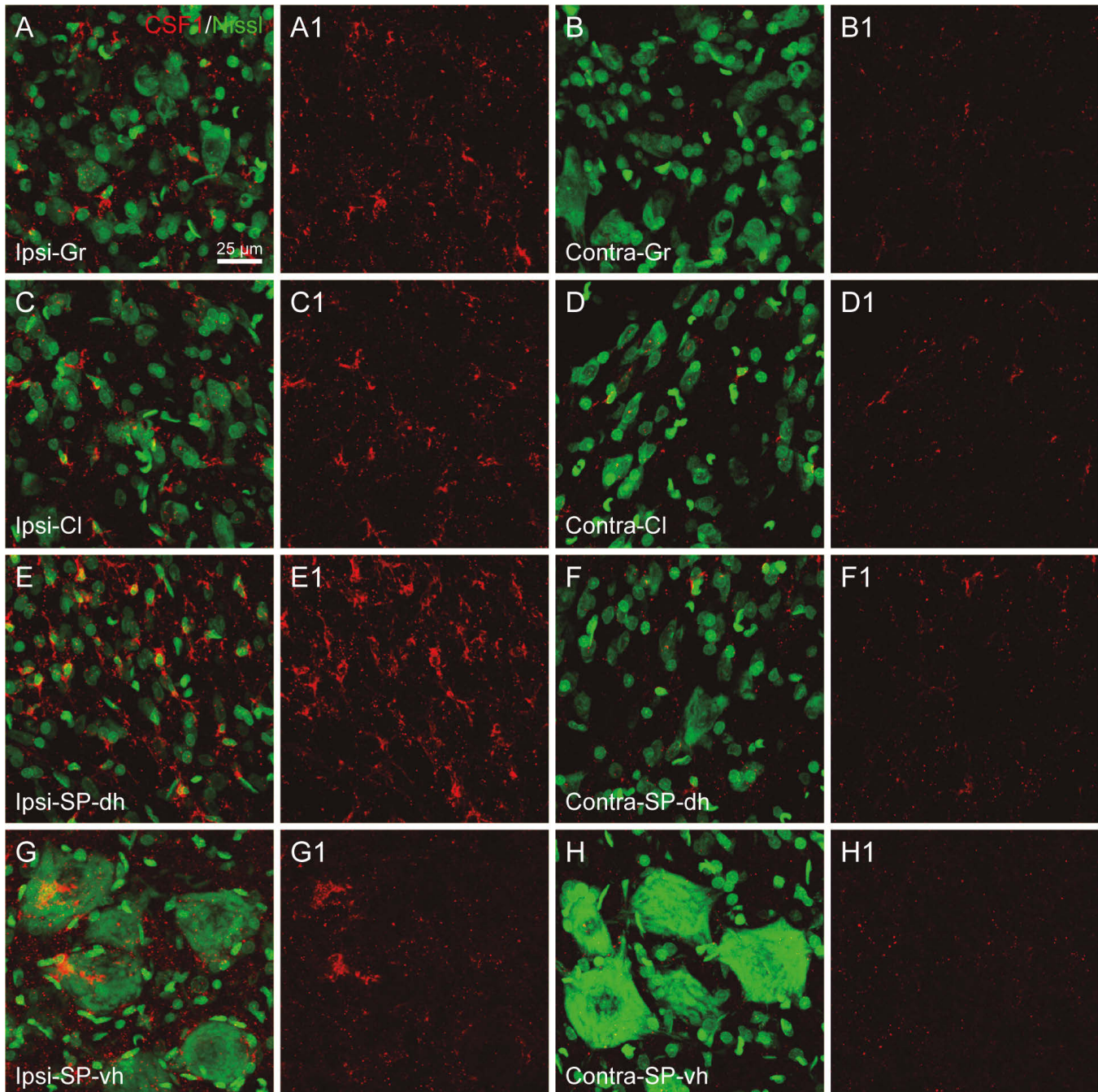


**Fig. 5.** Regional differences in CSF1 between the bilateral central sensory and motor territories of the lysophosphatidylcholine injured sciatic nerve. **A-H.** Representative images from bilateral sides of the gracile nucleus (**A, B**), Clarke's nucleus (**C, D**), spinal dorsal horn (**E, F**), and spinal ventral horn (**G, H**) showing CSF1 on the ipsilateral (**A, C, E, G**) and contralateral side (**B, D, F, H**) of lysophosphatidylcholine injury. **A1-H1.** Images separated from Figures A-H show CSF1 expression independently. CSF1: colony-stimulating factor 1. Same scale for all images.

### Spatial correlation of activated microglial cells and neurons

On the basis of the above observations, the spatial correlations of activated microglial cells and neurons were further examined with three-dimensional reconstruction (Fig. 6). On the spinal dorsal horn, although some activated microglial cell processes attached local neurons, most were separated between each other (Fig. 6A). Comparatively, on the spinal ventral horn, activated microglial cells located more closely to injured motor neurons, several activated microglial cells even simultaneously enwrapped a single injured motor neuron (Fig. 6B).

In addition, in contrast to crush injury, the sciatic nerve injured with LPC and transection led to microglial activation more obviously on the central sensory and motor territories of the sciatic nerve (Fig. 7).

### Discussion

With neural tract tracing and immunofluorescence staining techniques, we have mapped the central sensory and motor territories of the sciatic nerve, the region-specific response of central microglial cells to sciatic nerve demyelination, and the spatial correlation of activated microglial cells and neurons. Our results indicate that central microglial cells can be activated by sciatic nerve demyelination through both sensory and

motor pathways.

The neural tract tracing technique has been used for several decades to investigate neuronal connections (Köbber and Thanos, 2000; Vercelli et al., 2000; Lanciego and Wouterlood, 2011). As an important member of the tracer family, CTB is a sensitive tracer that specifically binds to the GM1 ganglioside on the surface of myelinated nerve fibers (Robertson and Grant, 1989). When applied peripherally, CTB is taken up by myelinated nerve fibers and retrogradely transported to motor neurons in the spinal ventral horn and sensory neurons in dorsal root ganglia. It can even be transported transganglionically to their central terminals in the gracile nucleus, Clarke's nucleus, and spinal dorsal horn (Rivero-Melián et al., 1992; Bosco and Poppele, 2001; Beggs and Salter, 2007; Xu et al., 2021). Along with the previous studies, here, we successfully labeled the central sensory and motor territories of the sciatic nerve with CTB, providing a topographic map that allowed us to evaluate whether microglial cells were activated by sciatic nerve demyelination through the neural pathway. This technique can also be potentially used for insights into the mechanisms underlying nerve injury and repair.

Since LPC was synthesized following nerve injury and converted to lysophosphatidic acid by autotaxin, subsequently leading to demyelination, the injection of LPC under the epineurium of the sciatic nerve has been widely used to establish a model of peripheral nerve demyelination (Inoue et al., 2008). Previous studies

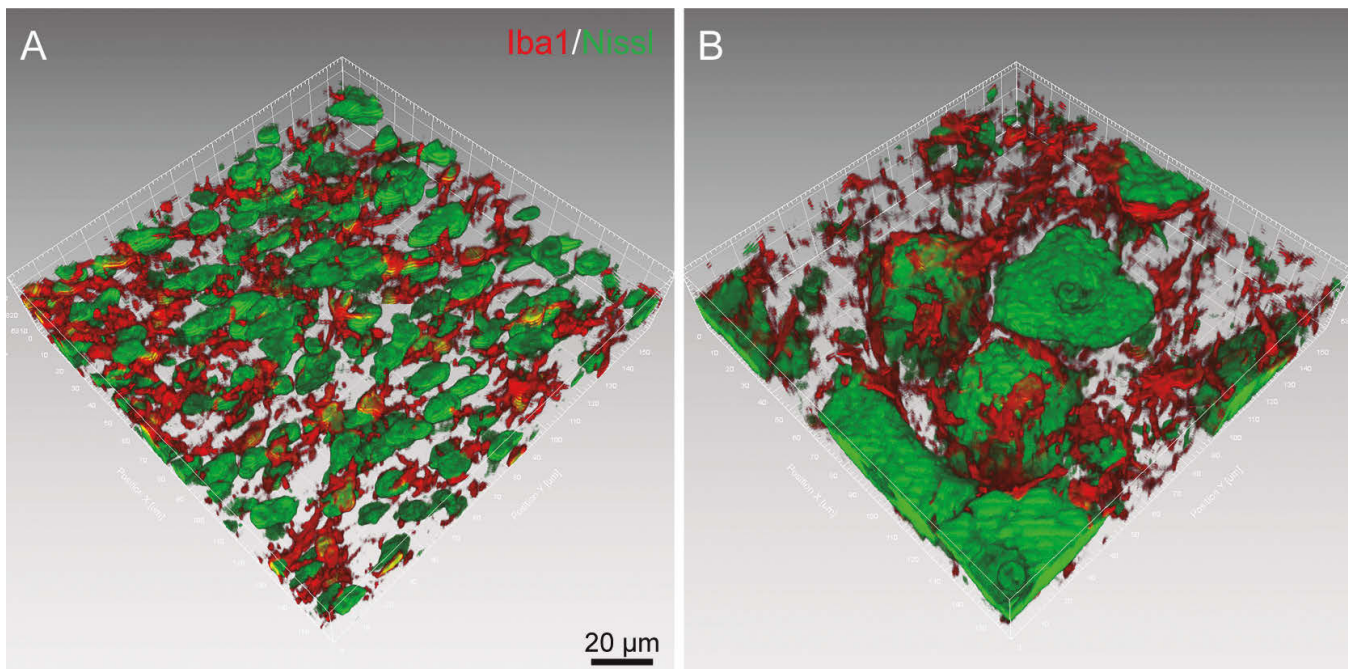


**Fig. 6.** Spatial correlation of activated microglial cells and neurons within the central sensory and motor territories of the lysophosphatidylcholine injured sciatic nerve. **A, B.** Representative adjusted images showing the three-dimensional views of activated microglial cells and neurons in the spinal dorsal horn (**A**) and spinal ventral horn (**B**) on the ipsilateral side of sciatic nerve demyelination. Iba1: ionized calcium-binding adapter molecule 1. Same scale for A and B.

### Microglial activation to nerve injury

primarily focused on using this model to investigate peripheral nerve remyelination and neuropathic pain (Inoue et al., 2008; Nagai et al., 2010; Nishimoto et al., 2015; Matsuoka et al., 2018). By this study, we further prove that LPC can also induce central microglial activation around injured motor neurons. In parallel with the various kinds of models of sciatic nerve injury, such as chronic constriction, transection and crush (Casals-Díaz et al., 2009; Geuna, 2015; Campos et al., 2021; Siwei et al., 2022), LPC-induced peripheral nerve demyelination can also be a valuable candidate for investigating central microglial activation in response to injured sensory afferents and motor neurons following peripheral nerve injury.

Microglial cells, the immune cells of the central nervous system, are capable of monitoring the microenvironment and responding to peripheral insults by transitioning from a resting to an activated state, accompanied by noticeable morphological changes (Svensson et al., 1993; Aldskogius, 2011; Pottorf et al., 2022). In the context of sciatic nerve demyelination, we observed that the distribution of activated microglial cells and upregulated CSF1 expression within the central sensory and motor territories was highly consistent with that of CTB labeling. This consistently supports the idea that central microglial cells were activated by sciatic nerve demyelination through both sensory and motor pathways transganglionically and retrogradely. Most studies on peripheral nerve injury have suggested that

central microglial activation may be associated with neuronal protection, degeneration, regeneration, synaptic plasticity, and spinal circuit reorganization (Svensson et al., 1993; Rotterman et al., 2019; Alvarez et al., 2020; Molnár et al., 2022; Pottorf et al., 2022). However, whether this activation plays detrimental or beneficial roles is still a subject to be further investigated (Hanisch and Kettenmann, 2007; Kettenmann et al., 2011; Pósfai et al., 2019; Pottorf et al., 2022).

As the incidence of peripheral demyelinating diseases is much higher in men, such as Guillain-Barre Syndrome, chronic inflammatory demyelinating polyneuropathy (Leonhard et al., 2019; Rodríguez et al., 2019; Shahrizaila et al., 2021), male SD rats were selected in this study. It should be emphasized that the central microglial activation observed in this preliminary study was limited to a single time-point following sciatic nerve demyelination. Therefore, our results do not provide a comprehensive understanding of the temporal kinetics of central microglial activation following this injury (Kohno et al., 2018). Further research is necessary to fully elucidate the dynamic changes sequentially (Kohno et al., 2018; Rotterman and Alvarez, 2020; Andoh and Koyama, 2021). In addition, due to the limited number of animals used in this study, our observations mainly focused on the morphological alterations of microglial cells. It is worth mentioning that, while injured motor neurons can be visualized using Nissl staining, central sensory terminals cannot be labeled with this method. Therefore, it limited

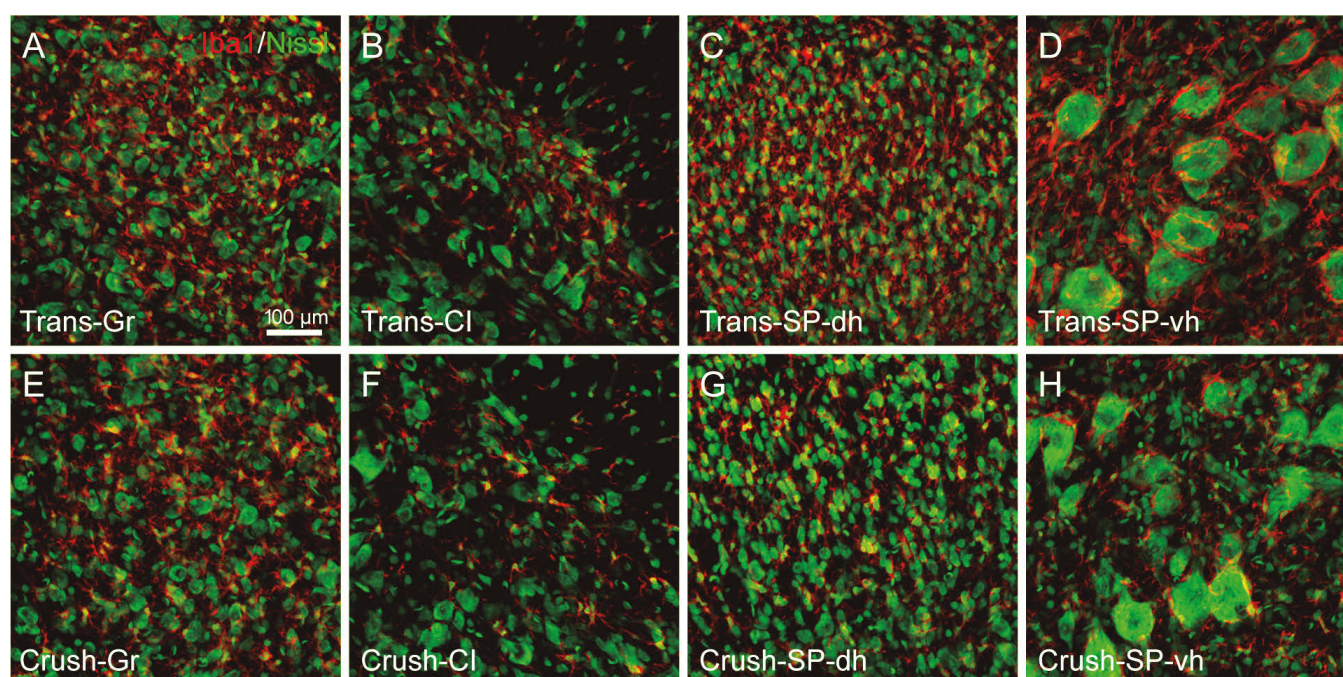


**Fig. 7.** Regional distribution of microglial cells in the central sensory and motor territories of the sciatic nerve under conditions of transection or crush injury. **A-H.** Representative images from the gracile nucleus (**A, E**), Clarke's nucleus (**B, F**), spinal dorsal horn (**C, G**), and spinal ventral horn (**D, H**) showing activated microglial cells on the ipsilateral side of transection (**Trans**) (**A-D**) and crush injury (**E-H**). Same scale for all images.

our observation of the potential “cross-talk” between activated microglial cells and central sensory terminals within the gracile nucleus, Clarke’s nucleus, and spinal dorsal horn.

### Conclusions

With the aid of neural tract tracing, immunofluorescence staining, and image reconstruction techniques, we provide a detailed morphological view of microglial activation in response to sciatic nerve demyelination through both sensory and motor pathways, which will facilitate the development of more effective treatment strategies for peripheral nerve demyelination from the perspective of central microglial-neuronal interactions.

*Acknowledgements, including funding sources.* This study was supported by the National Natural Science Foundation of China (No. 81774432); the CACMS Innovation Fund (No. CI2021A03407); and the Fundamental Research Funds for the Central Public Welfare Research Institutes of China (No. ZZ13-YQ-068, ZZ14-YQ-032, ZZ14-YQ-034).

*A conflict-of-interest statement.* Authors declare no conflicts of interest.

### References

- Aldskogius H. (2011). Mechanisms and consequences of microglial responses to peripheral axotomy. *Front. Biosci. (Schol Ed)*, 3, 857-868.
- Alvarez F.J., Rotterman T.M., Akhter E.T., Lane A.R., English A.W. and Cope T.C. (2020). Synaptic plasticity on motoneurons after axotomy: A necessary change in paradigm. *Front. Mol. Neurosci.* 30, 68.
- Andoh M. and Koyama R. (2021). Assessing microglial dynamics by live imaging. *Front. Immunol.* 12, 617564.
- Beggs S. and Salter M.W. (2007). Stereological and somatotopic analysis of the spinal microglial response to peripheral nerve injury. *Brain Behav. Immun.* 21, 624-633.
- Bosco G. and Poppele R.E. (2001). Proprioception from a spinocerebellar perspective. *Physiol. Rev.* 81, 539-568.
- Campos R.M.P., Barbosa-Silva M.C. and Ribeiro-Resende V.T. (2021). Comparison of effect of crush or transection peripheral nerve lesion on lumbar spinal cord synaptic plasticity and microglial dynamics. *IBRO. Neurosci. Rep.* 10, 225-235.
- Casals-Díaz L., Vivó M. and Navarro X. (2009). Nociceptive responses and spinal plastic changes of afferent C-fibers in three neuropathic pain models induced by sciatic nerve injury in the rat. *Exp. Neurol.* 217, 84-95.
- Eriksson N.P., Persson J.K., Svensson M., Arvidsson J., Molander C. and Aldskogius H. (1993). A quantitative analysis of the microglial cell reaction in central primary sensory projection territories following peripheral nerve injury in the adult rat. *Exp. Brain Res.* 96, 19-27.
- Geuna S. (2015). The sciatic nerve injury model in pre-clinical research. *J. Neurosci. Methods* 243, 39-46.
- Hanisch U.K. and Kettenmann H. (2007). Microglia: active sensor and versatile effector cells in the normal and pathologic brain. *Nat. Neurosci.* 10, 1387-1394.
- Inoue M., Xie W., Matsushita Y., Chun J., Aoki J. and Ueda H. (2008). Lysophosphatidylcholine induces neuropathic pain through an action of autotaxin to generate lysophosphatidic acid. *Neuroscience* 152, 296-298.
- Kettenmann H., Hanisch U.K., Noda M. and Verkhratsky A. (2011). Physiology of microglia. *Physiol. Rev.* 91, 461-553.
- Köbber C. and Thanos S. (2000). Topographic representation of the sciatic nerve motor neurons in the spinal cord of the adult rat correlates to region-specific activation patterns of microglia. *J. Neurocytol.* 29, 271-283.
- Kohno K., Kitano J., Kohro Y., Tozaki-Saitoh H., Inoue K. and Tsuda M. (2018). Temporal kinetics of microgliosis in the spinal dorsal horn after peripheral nerve injury in rodents. *Biol. Pharm. Bull.* 41, 1096-1102.
- Lanciego J.L. and Wouterlood F.G. (2011). A half century of experimental neuroanatomical tracing. *J. Chem. Neuroanat.* 42, 157-183.
- Leonhard S.E., Mandarakas M.R., Gondim F.A.A., Bateman K., Ferreira M.L.B., Cornblath D.R., van Doorn P.A., Dourado M.E., Hughes R.A.C., Islam B., Kusunoki S., Pardo C.A., Reisin R., Sejvar J.J., Shahrizaila N., Soares C., Umapathi T., Wang Y., Yiu E.M., Willison H.J. and Jacobs B.C. (2019). Diagnosis and management of Guillain-Barré syndrome in ten steps. *Nat. Rev. Neurol.* 15, 671-683.
- Matsuoka H., Tanaka H., Sayanagi J., Iwahashi T., Suzuki K., Nishimoto S., Okada K., Murase T. and Yoshikawa H. (2018). Neurotrophin® accelerates the differentiation of schwann cells and remyelination in a rat lysophosphatidylcholine-Induced demyelination model. *Int. J. Mol. Sci.* 19, 516.
- Molnár K., Nógrádi B., Kristóf R., Mészáros Á., Pajer K., Siklós L., Nógrádi A., Wilhelm I. and Krizbai I.A. (2022). Motoneuronal inflammasome activation triggers excessive neuroinflammation and impedes regeneration after sciatic nerve injury. *J. Neuroinflammation* 19, 68.
- Nagai J., Uchida H., Matsushita Y., Yano R., Ueda M., Niwa M., Aoki J., Chun J. and Ueda H. (2010). Autotaxin and lysophosphatidic acid1 receptor-mediated demyelination of dorsal root fibers by sciatic nerve injury and intrathecal lysophosphatidylcholine. *Mol. Pain* 6, 78.
- Nishihara T., Tanaka J., Sekiya K., Nishikawa, Y., Abe N., Hamada T., Kitamura S., Ikemune K., Ochi S., Choudhury M.E., Yano H. and Yorozuya T. (2020). Chronic constriction injury of the sciatic nerve in rats causes different activation modes of microglia between the anterior and posterior horns of the spinal cord. *Neurochem. Int.* 134, 104672.
- Nishimoto S., Tanaka H., Okamoto M., Okada K., Murase T. and Yoshikawa H. (2015). Methylcobalamin promotes the differentiation of Schwann cells and remyelination in lysophosphatidylcholine-induced demyelination of the rat sciatic nerve. *Front. Cell. Neurosci.* 9, 298.
- Paxinos G. and Watson C. (2007). The rat brain in stereotaxic coordinates. 6th ed. Academic Press. San Diego. pp 447-451.
- Pósfai B., Cserép C., Orsolits B. and Dénes Á. (2019). New insights into microglia-neuron interactions: a neuron’s perspective. *Neuroscience* 405, 103-117.
- Pottorf T.S., Rotterman T.M., McCallum W.M., Haley-Johnson Z.A. and Alvarez F.J. (2022). The role of microglia in neuroinflammation of the spinal cord after peripheral nerve injury. *Cells* 11.
- Rivero-Melián C., Rosario C., and Grant G. (1992). Demonstration of transganglionically transported cholera toxin in rat spinal cord by immunofluorescence cytochemistry. *Neurosci. Lett.* 145, 114-117.
- Robertson B. and Grant G. (1989). Immunocytochemical evidence for the localization of the GM1 ganglioside in carbonic anhydrase-

*Microglial activation to nerve injury*

- containing and RT 97-immunoreactive rat primary sensory neurons. *J. Neurocytol.* 18, 77-86.
- Rodríguez Y., Vatti N., Ramírez-Santana C., Chang C., Mancera-Páez O., Gershwin M.E. and Anaya J.M. (2019). Chronic inflammatory demyelinating polyneuropathy as an autoimmune disease. *J. Autoimmun.* 102, 8-37.
- Rotterman T.M., Akhter E.T., Lane A.R., MacPherson K.P., García V.V., Tansey M.G. and Alvarez F.J. (2019). Spinal motor circuit synaptic plasticity after peripheral nerve injury depends on microglia activation and a CCR2 mechanism. *J. Neurosci.* 39, 3412-3433.
- Rotterman T.M. and Alvarez F.J. (2020). Microglia dynamics and interactions with motoneurons axotomized after nerve injuries revealed by two-photon imaging. *Sci. Rep.* 10, 8648.
- Siwei Q., Ma N., Wang W., Chen S., Wu Q., Li Y. and Yang Z. (2022). Construction and effect evaluation of different sciatic nerve injury models in rats. *Transl. Neurosci.* 13, 38-51.
- Shahrizaila N., Lehmann H.C. and Kuwabara S. (2021). Guillain-Barré syndrome. *Lancet.* 397, 1214-1228.
- Svensson M., Eriksson P., Persson J.K., Molander C., Arvidsson J. and Aldskogius H. (1993). The response of central glia to peripheral nerve injury. *Brain. Res. Bull.* 30, 499-506.
- Vercelli A., Repici M., Garbossa D. and Grimaldi A. (2000). Recent techniques for tracing pathways in the central nervous system of developing and adult mammals. *Brain. Res. Bull.* 51, 11-28.
- Wang J., Xu D.S., Cui J.J., Wang S.Y., She C., Wang H., Wu S., Zhang J.L., Zhu B. and Bai W.Z. (2020). A new approach for examining the neurovascular structure with phalloidin and calcitonin gene-related peptide in the rat cranial dura mater. *J. Mol. Histol.* 51, 541-548.
- Wang J., Guo Y.T., Xu D.S., Cui J.J., Wang Y.Q., Su Y.X., Liu Y.H., Shen Y., Jing X.H. and Bai W.Z. (2022). The immunolocalization of cluster of differentiation 31, phalloidin and alpha smooth muscle actin on vascular network of normal and ischemic rat brain. *Sci. Rep.* 12, 22288.
- Wright G.D. and Horn H.F. (2016). Three-dimensional image analysis of the mouse cochlea. *Differentiation* 91, 104-108.
- Wu S., Wang J., Xu D.S., Su Y.X., Wang H., Zou L., Shen Y., Guo Y.T., Cui J.J. and Bai W.Z. (2021). Neural interconnection of acupuncture point “Chéngshān” (BL57) and sciatic nerve in the rat. *World J. Acupuncture-Moxibustion* 31, 129-135.
- Xu D.S., Zou L., Zhang W.J., Liao J.Y., Wang J., Cui J.J., Su Y.X., Wang Y.Q., Guo Y.T., Shen Y. and Bai W.Z. (2021). Comparison of sensory and motor innervation between the acupoints LR3 and LR8 in the rat with regional anatomy and neural tract tracing. *Front. Integr. Neurosci.* 15, 728747.

Accepted November 28, 2023